RESEARCH ARTICLE

Highly Accurate Analytical Approximate Solutions of the Electrostatically Actuated Parallel Plates

W. J. LIU AND X. Q. ZHAO

College of Mathematics and Computer, Jilin Normal University, Siping 136000, China

Corresponding author: W. J. Liu (2009003@jlnu.edu.cn)

ABSTRACT This paper is concerned with highly accurate analytical approximate solutions to dynamic oscillation of the parallel-plates model of an electrostatic micro-actuator. A potential difference is applied between the two electrodes to obtain a desired oscillatory effect, and the top movable electrode is suspended over the bottom fixed electrode by a linear suspension. The periodic oscillation solutions are obtained by generalizing the second-order Newton-harmonic balance (HB) method. The procedure obtains brief and accurate analytical approximate solutions for a large range of oscillation amplitudes with only one iteration step, the analytical approximate solutions show excellent agreement with the ''exact'' solution yielded by numerical integration. These analytical approximate solutions can be applied to analyze and design micro- and nano-devices employing electrostatic parallel plates.

INDEX TERMS Parallel plate, MEMS, analytical approximation, second-order Newton iteration, harmonic balance.

I. INTRODUCTION

Parallel plates are widely used as a necessary component in many microdevices that use electrostatic forces for actuation and capacitance changes for inspection. In bio-MEMS applications, the parallel plates act as micro-actuators for driving micropumps [1], [2] and microvalves [3]. In optical and RF MEMS applications, parallel plates are also applied to modulating a light beam [4], cantilever micro-electro-mechanical actuator [5], and even tuning a capacitance [6].

Due to the different geometry of the movable plates and flexures, the parallel plate suspended by flexures and subject to electric force moves toward the fixed plate with or without angular displacement. Parallel plate without angular displacement [7] is selected as a simple model in many MEMS device or component researches. A parallel-plate model is the one-dimensional idealization of an electrostatic micro actuator that is used to develop insight into its nonlinear dynamic behaviors [8], [9], [10]. For the parallel plate whose movable plate moves downward to the lower electrode, the pull-in voltage and the corresponding displacement were obtained in closed forms [8]. In addition, the effective stiffness, inter-

The associate editor coordinating the review of this manuscript and approving it for publication was Ming Xu.

plate gap, capacitance, resonant frequency and their sensitivities have also been derived as functions of the voltage applied across the plates [9]. In some MEMS devices, electrostatically actuated micro cantilever or fixed–fixed beam are simulated as a single parallel plate capacitor suspended by an ideal linear spring [11], [12], and obtained the behavior or response to an applied voltage by numerically solving a fourth-order nonlinear differential equation. Optimization [13], dynamic model development [14], or control [15] of a variety of parallel plates is concerned by researchers. On the other hand, electric membrane parallel plate [16] has been analyzed to examine the response to a given voltage. All parallel plates [7], [8], [9], [10], [11], [12], [13], [14], [15], [16] are nonlinear systems whose mechanical behavior is coupled with electrostatic forces generated by an applied voltage, so that the parallel plate's responses such as displacement at the voltage has been obtained by employing complicated numerical simulations. For further analytical studies of the parallel plate model, analytical approximate solutions which provide accurate explicit expressions of the model are attractive. Lee [9] derived a closed-form solution and a standard formula for a parallel-plate problem, which involved a movable rigid plate and a symmetrically-bent plate, and achieved a closed-form solution which included parameters such as the height of
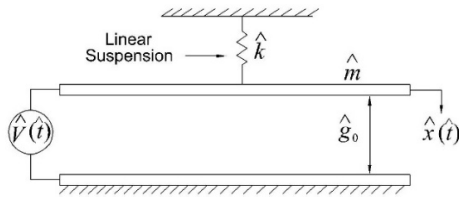
FIGURE 1. Schematic illustration of parallel-plates model for an electrostatic actuator.

TABLE 1. Parameters of the parallel-plate model.

Parameter	Value	Unit
$\hat{m}$	3.29×10^{-10}	kg
$\hat{k}$	476	N/m
$\hat{\varepsilon}_0$	8.85×10^{-12}	F/m
$\hat{A}$	6.2×10^{-8}	m²
$\hat{g}_0$	2×10^{-6}	m

the moving plate and its effective stiffness due to the applied voltage. Yu et al. [17] discussed the static and dynamic pull-in parameters of the parallel-plate microelectrostatic actuator with the help of Galerkin's method and Newton's method.

Nonlinear free vibration of a parallel-plates model that is subjected to constant voltage is investigated here. Although the second order Newton-HB method [18], [19] has been successful in some cases above, it is still a great challenge to extend and generalize this method to this parallel-plates vibration system. As it will become clearer below, this is because the governing equation does not only have concurrent presence of odd and non-odd nonlinear terms, but also contains highly negative-powered restoring terms. The coexistence of these terms makes the system extremely nonlinear, and hence, higher order approximation and assurance of numerical accuracy will become a challenge. Based on the nonlinear problem with odd and even nonlinearities, two new nonlinear equations with odd nonlinearity are proposed. The accurate analytical approximations of the original nonlinear problem are mathematically formulated by combining piecewise approximate solutions from such two new nonlinear systems. The details of modeling and approximations are presented below. In the illustrative examples specified by certain material parameters and initial conditions, the approximate analytical solutions are derived and subsequently verified by separately comparing to numerical integration solutions.

II. FORMULATION OF PARALLEL-PLATES MODEL
Consider a parallel-plates model as shown in Figure 1. The top movable electrode has mass $\hat{m}$, and is suspended over the bottom fixed electrode by a linear suspension having stiffness $\hat{k}$. The initial separation between the two electrodes is equal to $\hat{g}_0$. Permittivity of the vacuum is denoted by $\hat{\varepsilon}_0$ and $\hat{A}$ represents the area of overlap between the two electrodes, and $\hat{V}$ is the applied voltage. Also, $\hat{x}(\hat{t})$ denotes the time-dependent displacement of the movable electrode. Parameters of the parallel-plate model are list in Table 1.

Neglecting the effect of energy dissipation, the dynamic equation of motion of the system is written as

$$\hat{m}\frac{d^2\hat{x}}{d\hat{t}^2} + \hat{k}\hat{x} = \frac{\hat{\varepsilon}_0\hat{A}\hat{V}^2}{2\left(\hat{g}_0 - \hat{x}\right)^2},$$

$$\hat{x}(0) = 0, \frac{d\hat{x}}{d\hat{t}}(0) = 0. \tag{1}$$

We define the following dimensionless quantities in order to generalize the forthcoming analysis:

$$x(t) = \frac{\hat{x}(\hat{t})}{\hat{g}_0}, V = \left(\frac{\hat{\varepsilon}_0\hat{A}\hat{V}^2}{\hat{k}\hat{g}_0^3}\right)^{\frac{1}{2}}, t = \left(\frac{\hat{k}}{\hat{m}}\right)^{\frac{1}{2}}\hat{t} \tag{2}$$

where x, V, and t denote normalized displacement, dimensionless voltage and dimensionless time, respectively. These definitions reduce (1) to the following dimensionless form [10]:

$$\frac{d^2x}{dt^2} + x = \frac{V^2}{2(1-x)^2}, x(0) = 0, \frac{dx}{dt}(0) = 0. \tag{3}$$

Then, (3) can be rewritten as

$$\frac{d^2x}{dt^2} + F(x, V) = 0,$$

where

$$F(x, V) = x - \frac{V^2}{2(1-x)^2}.$$

III. ANALYTICAL APPROXIMATIONS TO STATIC PULL-IN STATE
Setting the time derivatives in (3) to zero, assuming a constant electric load yields the nonlinear algebraic equation governing the static deflection as of the parallel-plate as follows

$$F(x_s, V) = x_s - \frac{V^2}{2(1-x_s)^2} = 0. \tag{4}$$

Based on (4), the potential V ($V \geq 0$) can be solved and expressed in terms of the normalized static beam center

$$V = \sqrt{2(1-x_s)^2x_s}. \tag{5}$$

In general, the solution curve in (5) is composed of the left and right branches. In figure 2, the highest point is the pull-in one where the corresponding voltage and normalized static beam-center deflection are denoted by Vp and xp, respectively. In addition, stability analyses of the static deflection have been performed in [20]. It has been pointed that, the left branch is stable and the right branch is unstable. The static pull-in parameters (normalized voltage Vp and normalized displacement x_s) of the plates are derived by (5), $xp = 1/3$, $Vp = 0.544331$.

IV. ANALYTICAL APPROXIMATIONS TO NONLINEAR FREE VIBTATIONS
In this section, we construct the analytical approximate periods and periodic solutions to (3). Let deflection
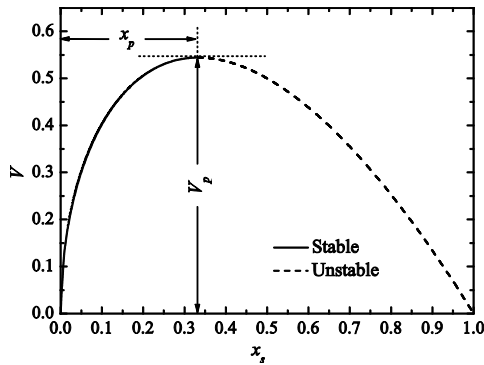
$$x = x_s + u, \tag{6}$$

FIGURE 2. Variation of normalized voltage V along with normalized static deflection x_S.
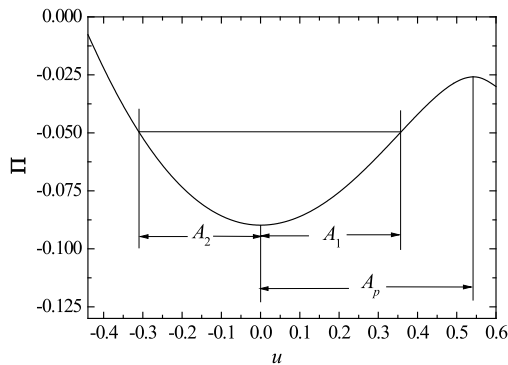

FIGURE 3. Variation of the potential energy $\prod$ with normalized incremental deflection u for $x_S = 0.1$.

where u is the normalized incremental deflection from a stable equilibrium position $x = x_s$. Substituting (6) into (3) leads to

$$\frac{d^2u}{dt^2} + f(u) = 0, u(0) = A_1, \frac{du}{dt}(0) = 0. \quad (7)$$

where

$$f(u) = x_s + u - \frac{V^2}{2(1 - x_s - u)^2}, V = V(x_s), A_1 = A - x_s.$$

and A_1 represents the initial normalized maximum displacement. The corresponding potential energy function is

$$\prod(u, V) = \int f(u)\,du = \frac{u^2}{2} + ux_s - \frac{V^2}{2(1 - u - x_s)}, \quad (8)$$

and it reaches its minimum at $u = 0$. Thus, the system will oscillate between asymmetric limits $[-A_2, A_1]$ where both $-A_2 (A_2 > 0)$ and A_1 have the same energy level, namely

$$\prod(-A_2, V) = \prod(A_1, V), \quad (9)$$

and they are left and right limitations of normalized incremental deflection, respectively, for the vibration. In figure 3 the change of the potential energy $\prod(u, V) (x_s = 0.1)$ with respect to the normalized incremental deflection u is shown.

The denominator of elelectrostatic force is expended into a Taylor series at $u = 0$ up to the third order. Further, (7) is approximated by

$$\frac{d^2u}{dt^2} + \frac{C_1u + C_2u^2 + u^3}{M_0 + M_1u + u^2} = 0, u(0) = A_1, \frac{du}{dt}(0) = 0. \quad (10)$$

where

$$C_1 = 1 - 4x_s + 3x_s^2, C_2 = 3x_s - 2, M_0$$
$$= 1 - 2x_s + x_s^2, M_1 = 2x_s - 2.$$

Introducing the new independent variable $\tau = \omega t$, we may transform (10) as

$$\Omega\left(M_0 + M_1u + u^2\right)\ddot{u} + C_1u + C_2u^2 + u^3 = 0,$$
$$u(0) = A_1, \dot{u}(0) = 0. \quad (11)$$

where $\Omega = \omega^2$ and a dot denotes differentiation with respect to τ. Based on (11), two odd nonlinear oscillators for $i = 1, 2$ are defined as follows

$$\Omega_i\Phi^{(i)}(u)\ddot{u} + K^{(i)}(u)$$
$$= 0, u(0) = A_i, \dot{u}(0) = 0, \quad (12a)$$

$$\Phi^{(i)}(u) = \begin{cases} M_0 + (-1)^{i-1}M_1u + u^2, & \text{if } u \geq 0, \\ M_0 - (-1)^{i-1}M_1u + u^2, & \text{if } u < 0. \end{cases} \quad (12b)$$

$$K^{(i)}(u) = \begin{cases} C_1u + (-1)^{i-1}C_2u^2 + u^3, & \text{if } u \geq 0, \\ C_1u - (-1)^{i-1}C_2u^2 + u^3, & \text{if } u < 0. \end{cases} \quad (12c)$$

Here, for $i = 1, 2$, $K^{(i)}(u)$ is an odd function of u, and $\Phi^{(i)}(u)$ is an even function of u.

Based on the single term HB method, the initial approximation to (12) is set as

$$u_1^{(i)} = A_i \cos \tau, i=1,2 \quad (13)$$

Substituting (13) into (12), expanding the resulting expression in the Fourier series and setting the coefficient of $\cos \tau$ to zero result in

$$\Omega_1^{(i)}(A_i) = \frac{9\pi A_i^2 + 12\pi C_1 + 32(-1)^{i-1}A_iC_2}{9\pi A_i^2 + 12\pi M_0 + 32(-1)^{i-1}A_iM_1}, i = 1, 2 \quad (14)$$

Therefore, the first approximation to the period of nonlinear oscillator in (12) for $i = 1, 2$ is

$$T_1^{(i)}(A_i) = 2\pi \left/ \sqrt{\Omega_1^{(i)}(A_i)}, \right. \quad (15)$$

and the corresponding approximate periodic solution is

$$u_1^{(i)}(t) = A_i \cos\left(\sqrt{\Omega_1^{(i)}(A_i)}t\right). \quad (16)$$

Based on the initial approximations $\Omega_1^{(i)}(A_i)$ and $u_1^{(i)}(t)$ in (14) and (16), respectively, to the solution of (12), the second-order Taylor expansion and the HB method can be combined to obtain a more accurate solution. The periodic solution of (12) and its frequency squared can be formulated as

$$u^{(i)} = u_1^{(i)} + \Delta u_1^{(i)}, \Omega^{(i)} = \Omega_1^{(i)} + \Delta\Omega_1^{(i)}, i = 1, 2 \quad (17)$$

Substituting (17) into (12), neglecting the third-order and higher-order power degree terms in $\Delta u_1^{(i)}$ and $\Delta\Omega_1^{(i)}$, lead to

$$\Phi^{(i)}(u_1^{(i)})\left(\Omega_1^{(i)}\ddot{u}_1^{(i)} + \Delta\Omega_1^{(i)}\ddot{u}_1^{(i)} + \Omega_1^{(i)}\Delta\ddot{u}_1^{(i)} + \Delta\Omega_1^{(i)}\Delta\ddot{u}_1^{(i)}\right)$$

$$+ \Phi_u^{(i)}(u_1^{(i)})\Delta u_1^{(i)}\left(\Omega_1^{(i)}\ddot{u}(i)_1^{(i)} + \Delta\Omega_1^{(i)}\ddot{u}_1^{(i)} + \Omega_1^{(i)}\Delta\ddot{u}_1^{(i)}\right)$$
$$+ K^{(i)}(u_1^{(i)}) + K_u^{(i)}(u_1^{(i)})\Delta u_1^{(i)}$$
$$+ \frac{1}{2}\left[\Phi_{uu}^{(i)}(u_1^{(i)})\Omega_1^{(i)}\ddot{u}_1^{(i)} + K_{uu}(u_1^{(i)})\right](\Delta u_1^{(i)})^2 = 0,$$
$$\Delta u_1^{(i)}(0) = 0, \Delta\dot{u}_1^{(i)}(0) = 0, i = 1, 2 \tag{18}$$

Firstly, the linearized equation in $\Delta u_{10}^{(i)}$ and $\Delta\Omega_{10}^{(i)}$ derived from (18)

$$\Omega_1^{(i)}\Phi^{(i)}(u_1^{(i)})\ddot{u}_1^{(i)} + K^{(i)}(u_1^{(i)}) + \Delta\Omega_{10}^{(i)}\Phi^{(i)}(u_1^{(i)})\ddot{u}_1^{(i)}$$
$$+ \Omega_1^{(i)}\Phi^{(i)}(u_1^{(i)})\Delta\ddot{u}_{10}^{(i)} + \Omega_1^{(i)}\Phi_u^{(i)}(u_1^{(i)})\ddot{u}_1^{(i)}\Delta u_{10}^{(i)}$$
$$+ K_u^{(i)}(u_1^{(i)})\Delta u_{10}^{(i)} = 0,$$
$$\Delta u_{10}^{(i)}(0) = 0, \Delta\dot{u}_{10}^{(i)}(0) = 0, i = 1, 2 \tag{19}$$

is solved. The approximate solution to (19) can be developed by setting $\Delta u_{10}^{(i)}$ as

$$\Delta u_{10}^{(i)}(\tau) = \alpha_1^{(i)}(\cos\tau - \cos 3\tau), i = 1, 2 \tag{20}$$

Substituting (13) and (20) into (19), expanding the resulting expression into the Fourier series, setting the coefficients of $\cos\tau$ and $\cos 3\tau$ to zero, respectively, yield

$$\Omega_{10}^{(i)} = \frac{N_2^{(i)}P_\alpha^{(i)} - N_1^{(i)}Q_\alpha^{(i)}}{Q_\alpha^{(i)}P_\Omega^{(i)} - P_\alpha^{(i)}Q_\Omega^{(i)}}, \alpha^{(i)}$$
$$= \frac{-N_2^{(i)}P_\Omega^{(i)} + N_1^{(i)}Q_\Omega^{(i)}}{Q_\alpha^{(i)}P_\Omega^{(i)} - P_\alpha^{(i)}Q_\Omega^{(i)}}, \quad i = 1, 2. \tag{21}$$

where $P_\alpha^{(i)}, P_\Omega^{(i)}, N_j^{(i)}, Q_\alpha^{(i)},$ and $Q_\Omega^{(i)}, (i = 1, 2; j = 1, 2)$ are listed in Appendix VI.

Therefore, the second approximate period and periodic solution to (12) for $i = 1, 2$ can be expressed as

$$T_2^{(i)}(A_i) = 2\pi/\sqrt{\Omega_2^{(i)}(A_i)}, \tag{22}$$
$$u_2^{(i)}(\tau) = (A_i + \alpha_1^{(i)})\cos\left(\sqrt{\Omega_2^{(i)}(A_i)}t\right)$$
$$- \alpha_1^{(i)}\cos\left(3\sqrt{\Omega_2^{(i)}(A_i)}t\right), \tag{23}$$

where

$$\Omega_2^{(i)} = \Omega_1^{(i)} + \Delta\Omega_{10}^{(i)}. \tag{24}$$

Next, in (18), replacing $\Delta\Omega_1^{(i)}$ in $\Delta\Omega_1^{(i)}\Phi^{(i)}(u_1^{(i)})\Delta\ddot{u}_1^{(i)}$ with $\Delta\Omega_{10}^{(i)}, \Delta\ddot{u}_1^{(i)}$ in $\Omega_1^{(i)}\Phi_u^{(i)}(u_1^{(i)})\Delta\ddot{u}_1^{(i)}\Delta u_1^{(i)}$ with $\Delta\ddot{u}_{10}^{(i)}, \Delta\Omega_1^{(i)}$ in $\Delta\Omega_1^{(i)}\Phi_u^{(i)}\left(u_1^{(i)}\right)\ddot{u}_1^{(i)}\Delta u_1^{(i)}$ with $\Delta\Omega_{10}^{(i)}$, and one of two $\Delta u_1^{(i)}$ terms in $0.5(\Delta u_1^{(i)})^2\Omega_1^{(i)}\Phi_{uu}^{(i)}(u_1^{(i)})\ddot{u}_1^{(i)} + 0.5(\Delta u_1^{(i)})^2 K_{uu}^{(i)}(u_1^{(i)})$ with $\Delta u_{10}^{(i)}$, respectively, yields linear equation in $\Delta u_1^{(i)}$ and $\Delta\Omega_1^{(i)}$:

$$\Phi^{(i)}(u_1^{(i)})\left(\Omega_1^{(i)}\ddot{u}_1^{(i)} + \Delta\Omega_1^{(i)}\ddot{u}_1^{(i)} + \Omega_1^{(i)}\Delta\ddot{u}_1^{(i)} + \Delta\Omega_{10}^{(i)}\Delta\ddot{u}_{10}^{(i)}\right)$$
$$+ \Phi_u^{(i)}(u_1^{(i)})\Delta u_1^{(i)}\left(\Omega_1^{(i)}\ddot{u}_1^{(i)} + \Delta\Omega_{10}^{(i)}\ddot{u}_1^{(i)} + \Omega_1^{(i)}\Delta\ddot{u}_{10}^{(i)}\right)$$
$$+ K^{(i)}(u_1^{(i)}) + K_u^{(i)}(u_1^{(i)})\Delta u_1^{(i)}$$

$$+ \frac{1}{2}\left[\Phi_{uu}^{(i)}(u_1^{(i)})\Omega_1^{(i)}\ddot{u}_1^{(i)} + K_{uu}(u_1^{(i)})\right]\Delta u_{10}^{(i)}\Delta u_1^{(i)} = 0,$$
$$\Delta u_1^{(i)}(0) = 0, \Delta\dot{u}_1^{(i)}(0) = 0, i = 1, 2 \tag{25}$$

Let $\Delta u_1^{(i)}$ in (25) be

$$\Delta u_1^{(i)}(\tau) = \beta^{(i)}(\cos\tau - \cos 3\tau) + \gamma^{(i)}(\cos 3\tau - \cos 5\tau), \tag{26}$$

which satisfies the initial conditions in (25). Substituting (13), (14), (20), (21), and (26) into (25), expanding the resulting expression into the Fourier series and setting the coefficients of $\cos\tau$, $\cos 3\tau$ and $\cos 5\tau$ to zeros, respectively, produce, as in (27), shown at the bottom of the next page, where $R_\Omega^{(i)}, P_\beta^{(i)}, P_\gamma^{(i)}, N_k^{(i)}, E_\Omega^{(i)}, Q_\beta^{(i)}, Q_\gamma^{(i)}, F_\Omega^{(i)}, S_\beta^{(i)}$, and $S_\gamma^{(i)}(i = 1, 2; k = 1, 2, 3)$ are listed in Appendix VI.

Finally, the third approximations to the period and corresponding periodic solution to (12) for $i = 1, 2$ can be written as

$$T_3^{(i)}(A_i) = 2\pi/\sqrt{\Omega_3^{(i)}(A_i)}, \tag{28}$$
$$u_3^{(i)}(t) = \left(A_i + \beta^{(i)}\right)\cos\left[\sqrt{\Omega_3^{(i)}(A_i)}t\right]$$
$$+ \left(-\beta^{(i)} + \gamma^{(i)}\right)\cos\left[3\sqrt{\Omega_3^{(i)}(A_i)}t\right]$$
$$- \gamma^{(i)}\cos\left[5\sqrt{\Omega_3^{(i)}(A_i)}t\right], \tag{29}$$

where

$$\Omega_3^{(i)} = \Omega_1^{(i)} + \Delta\Omega_1^{(i)}. \tag{30}$$

Finally, the corresponding the nth $(n = 1, 2, 3)$ analytical approximate period and periodic solution to (7) can be written as

$$T_n(A_1) = \frac{T_n^{(1)}(A_1)}{2} + \frac{T_n^{(2)}(A_2)}{2}, \tag{31}$$

$$u_n(t) = \begin{cases} u_n^{(1)}(t), 0 \leq t \leq \frac{T_n^{(1)}(A_1)}{4}; \\ u_n^{(2)}\left(t - \frac{T_n^{(1)}(A_1)}{4} + \frac{T_n^{(2)}(A_2)}{4}\right), \\ \qquad \frac{T_n^{(1)}(A_1)}{4} \leq t \leq \frac{T_n^{(1)}(A_1)}{4} + \frac{T_n^{(2)}(A_2)}{2}; \\ u_n^{(1)}\left(t + \frac{T_n^{(1)}(A_1)}{2} - \frac{T_n^{(2)}(A_2)}{2}\right), \\ \qquad \frac{T_n^{(1)}(A_1)}{4} + \frac{T_n^{(2)}(A_2)}{2} \leq t \leq \frac{T_n^{(1)}(A)}{2} \\ \qquad + \frac{T_n^{(2)}(A_2)}{2} \end{cases} \tag{32}$$

The exact period $T_e(A_1)$ is

$$T_e(A_1) = 2\int_{-A_2}^{A_1}[2\Pi(A_1, V) - 2\Pi(A_2, V)]^{-1/2}du. \tag{33}$$

where A_2 is determined by (8) and (9).

TABLE 2. Comparison of approximate and "exact" periods for $x_S = 0.1$, $V = 0.402492$, $A_p = 0.545862$.

A_1	A_2	T_e	T_1/T_e	T_2/T_e	T_3/T_e
0.2	0.187117	7.23348	0.999020	1.00000	0.999997
0.3	0.269042	7.40651	0.996390	1.00005	0.999988
0.4	0.338365	7.77320	0.986783	1.00022	0.999934
0.5	0.384768	8.88811	0.932677	0.99615	0.998401
0.53	0.390802	10.1015	0.853854	0.968100	0.985228
0.54	0.391593	11.2971	0.775965	0.912984	0.946970

TABLE 3. Comparison of approximate and "exact" periods for $x_S = 0.2$, $V = 0.505964$, $A_p = 0.287689$.

A_1	A_2	T_e	T_1/T_e	T_2/T_e	T_3/T_e
0.1	0.088298	9.11837	0.998886	1.00002	0.999994
0.15	0.123554	9.45623	0.996344	1.00010	0.999977
0.2	0.151661	10.0898	0.988516	1.00044	0.999892
0.25	0.170297	11.5499	0.955292	1.00029	0.998937
0.27	0.174178	13.0211	0.904198	0.992108	0.993946
0.28	0.175143	14.7186	0.834185	0.962557	0.974238

TABLE 4. Comparison of approximate and "exact" periods for $x_S = 0.3$, $V = 0.542218$, $A_p = 0.0678175$.

A_1	A_2	T_e	T_1/T_e	T_2/T_e	T_3/T_e
0.01	0.009204	16.7459	0.999864	1.00001	1.00000
0.03	0.023473	17.7366	0.998118	1.0001	0.999981
0.05	0.032596	20.4903	0.985938	1.00073	0.999769
0.06	0.035000	24.1240	0.949856	0.999682	0.998142
0.065	0.035548	28.9753	0.871316	0.979444	0.984414
0.067	0.035628	35.0257	0.757845	0.906390	0.924609

V. RESULTS AND DISCUSSION

To describe the dynamic vibration behavior and verify the accuracy of analytical approximate solutions, comparative analysis of the approximate and "exact" solutions is given in this section.

The "exact" period $T_e(A_1)$ obtained by (33) and the approximate periods $T_1(A_1)$, $T_2(A_1)$, and $T_3(A_1)$ computed by (31) are listed in Table 2, 3, and 4. Note that the maximum amplitude Ap of vibration is determined by the difference between unstable deflection in the right branch and stable static deflection as in the left branch at an equal potential $V(x_s)$. From Table 2, 3, and 4, it can be analyzed that the third approximate period $T_3(A_1)$ derived by (33) provides
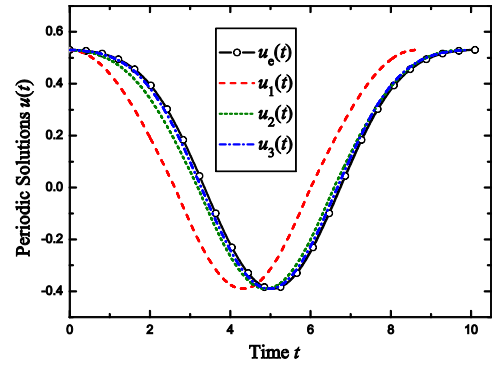

FIGURE 4. Comparison of approximate periodic solutions with "exact" solution for $x_S = 0.1$, $V = 0.402492$, $A_1 = 0.53$.
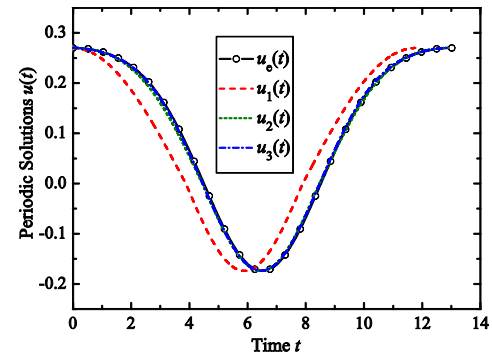

FIGURE 5. Comparison of approximate periodic solutions with "exact" solution for $x_S = 0.2$, $V = 0.505964$, $A_1 = 0.27$.
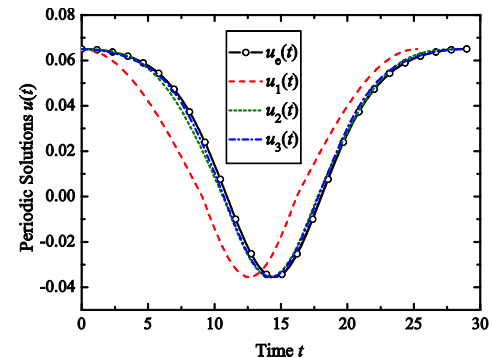

FIGURE 6. Comparison of approximate periodic solutions with "exact" solution for $x_S = 0.3$, $V = 0.542218$, $A_1 = 0.065$.

very good accuracy to the exact period for various vibration amplitudes.

$$\Delta\Omega_1^{(i)} = \frac{Q_\beta^{(i)} S_\gamma^{(i)} N_3^{(i)} - Q_\gamma^{(i)} S_\beta^{(i)} N_3^{(i)} + P_\gamma^{(i)} S_\beta^{(i)} N_4^{(i)} - P_\beta^{(i)} S_\gamma^{(i)} N_4^{(i)} - P_\gamma^{(i)} Q_\beta^{(i)} N_5^{(i)} + P_\beta^{(i)} Q_\gamma^{(i)} N_5^{(i)}}{F_\Omega^{(i)} P_\gamma^{(i)} Q_\beta^{(i)} - F_\Omega^{(i)} P_\beta^{(i)} Q_\gamma^{(i)} - E_\Omega^{(i)} P_\gamma^{(i)} S_\beta^{(i)} + Q_\gamma^{(i)} R_\Omega^{(i)} S_\beta^{(i)} + E_\Omega^{(i)} P_\beta^{(i)} S_\gamma^{(i)} - Q_\beta^{(i)} R_\Omega^{(i)} S_\gamma^{(i)}}$$

$$\beta^{(i)} = \frac{F_\Omega^{(i)} Q_\gamma^{(i)} N_3^{(i)} - E_\Omega^{(i)} S_\gamma^{(i)} N_3^{(i)} - F_\Omega^{(i)} P_\gamma^{(i)} N_4^{(i)} + R_\Omega^{(i)} S_\gamma^{(i)} N_4^{(i)} + E_\Omega^{(i)} P_\gamma^{(i)} N_5^{(i)} - Q_\gamma^{(i)} R_\Omega^{(i)} N_5^{(i)}}{F_\Omega^{(i)} P_\gamma^{(i)} Q_\beta^{(i)} - F_\Omega^{(i)} P_\beta^{(i)} Q_\gamma^{(i)} - E_\Omega^{(i)} P_\gamma^{(i)} S_\beta^{(i)} + Q_\gamma^{(i)} R_\Omega^{(i)} S_\beta^{(i)} + E_\Omega^{(i)} P_\beta^{(i)} S_\gamma^{(i)} - Q_\beta^{(i)} R_\Omega^{(i)} S_\gamma^{(i)}}$$

$$\gamma^{(i)} = \frac{E_\Omega^{(i)} S_\beta^{(i)} N_3^{(i)} - F_\Omega^{(i)} Q_\beta^{(i)} N_3^{(i)} + F_\Omega^{(i)} P_\beta^{(i)} N_4^{(i)} - R_\Omega^{(i)} S_\beta^{(i)} N_4^{(i)} - E_\Omega^{(i)} P_\beta^{(i)} N_5^{(i)} + Q_\beta^{(i)} R_\Omega^{(i)} N_5^{(i)}}{F_\Omega^{(i)} P_\gamma^{(i)} Q_\beta^{(i)} - F_\Omega^{(i)} P_\beta^{(i)} Q_\gamma^{(i)} - E_\Omega^{(i)} P_\gamma^{(i)} S_\beta^{(i)} + Q_\gamma^{(i)} R_\Omega^{(i)} S_\beta^{(i)} + E_\Omega^{(i)} P_\beta^{(i)} S_\gamma^{(i)} - Q_\beta^{(i)} R_\Omega^{(i)} S_\gamma^{(i)}} \tag{27}$$

For $x_s = 0.1, V = 0.402492, A_1 = 0.53$; $x_s = 0.2, V = 0.505964, A_1 = 0.27$, and $x_s = 0.3, V = 0.542218$, $A_1 = 0.065$ the "exact" periodic solution $u_e(t)$ calculated by numerically solving the initial value problem of (7) with the Runge-Kutta method and the approximate analytical periodic solutions $u_1(t)$, $u_2(t)$, and $u_3(t)$ computed by (32) are presented in figure 4, 5, and 6. These figures show that the second analytical approximate periodic solutions in (32) provide the very good approximations to the "exact" periodic solutions for the whole range of small and large amplitude of vibration.

VI. CONCLUSION
In this study, the nonlinear free vibration of the parallel-plate type microelectrostatic actuator is analytically investigated by combing the second-order Newton method and the harmonic balance method. The governing equation that is expressed in a specific form has been solved in two steps, a predictor step and a corrector step. Solution to each step has been constructed in an appropriate manner using the harmonic balance method. This new method retains the advantage of solving a set of linear equations instead of a set of nonlinear ones, yet it incorporates in a natural way the second-order terms in the expansion. This higher-order method yields accurate solutions with faster convergence rate for all amplitudes of the parallel-plate type microelectrostatic actuator. With these analytical expressions, it is possible to perform analytical parametric investigations with respect to various physical quantities that influence the dynamic behavior and to help MEMS and NEMS designers for improving the performances of resonant sensors.

APPENDIX A
The coefficients $P_\alpha^{(i)}$, $P_\Omega^{(i)}$, $N_j^{(i)}$, $Q_\alpha^{(i)}$, and $Q_\Omega^{(i)}$, $(i = 1, 2; j = 1, 2)$ in (21) are given by

$$P_\alpha^{(i)} = \frac{3A_i^2}{2} + C_1 + \frac{64(-1)^{i-1}A_iC_2}{15\pi} + \frac{1}{2}A_i^2\Omega_1^{(i)} - M_0\Omega_1^{(i)},$$

$$P_\Omega^{(i)} = -\frac{3A_i^3}{4} - A_iM_0 - \frac{8(-1)^{i-1}A_i^2M_1}{3\pi},$$

$$N_1^{(i)} = \frac{3A_i^3}{4} + A_iC_1 + \frac{8(-1)^{i-1}A_i^2C_2}{3\pi} - \frac{3}{4}A_i^3\Omega_1^{(i)}$$
$$- A_iM_0\Omega_1^{(i)} - \frac{8(-1)^{i-1}A_i^2M_1\Omega_1^{(i)}}{3\pi},$$

$$Q_\alpha^{(i)} = -\frac{3A_i^2}{4} - C_1 - \frac{64(-1)^{i-1}A_iC_2}{21\pi} + \frac{19}{4}A_i^2\Omega_1^{(i)}$$
$$+ 9M_0\Omega_1^{(i)} + \frac{2048(-1)^{i-1}A_iM_1\Omega_1^{(i)}}{105\pi},$$

$$Q_\Omega^{(i)} = -\frac{A_i^3}{4} - \frac{8(-1)^{i-1}A_i^2M_1}{15\pi},$$

$$N_2^{(i)} = \frac{A_i^3}{4} + \frac{8(-1)^{i-1}A_i^2C_2}{15\pi} - \frac{1}{4}A_i^3\Omega_1^{(i)}$$
$$- \frac{8(-1)^{i-1}A_i^2M_1\Omega_1^{(i)}}{15\pi}.$$

APPENDIX B
The coefficients $R_\Omega^{(i)}$, $P_\beta^{(i)}$, $P_\gamma^{(i)}$, $N_k^{(i)}$, $E_\Omega^{(i)}$, $Q_\beta^{(i)}$, $Q_\gamma^{(i)}$, $F_\Omega^{(i)}$, $S_\beta^{(i)}$, and $S_\gamma^{(i)}(i = 1, 2; k = 1, 2, 3)$ in (27) are given by

$$R_\Omega^{(i)} = -\frac{3A_i^3}{4} - A_iM_0 - \frac{8(-1)^{i-1}A_i^2M_1}{3\pi},$$

$$P_\beta^{(i)} = \frac{3A_i^2}{2} + C_1 + \frac{64(-1)^{i-1}A_iC_2}{15\pi} + \frac{9A_i\alpha_1^{(i)}}{4}$$
$$+ \frac{128(-1)^{i-1}C_2\alpha_1^{(i)}}{35\pi} + \frac{1}{2}A_i^2\Delta\Omega_{10}^{(i)} - M_0\Delta\Omega_{10}^{(i)}$$
$$+ \frac{1}{2}A_i^2\Omega_1^{(i)}$$
$$- M_0\Omega_1^{(i)} - \frac{11}{2}A_i\alpha_1^{(i)}\Omega_1^{(i)} - \frac{1664(-1)^{i-1}M_1\alpha_1^{(i)}\Omega_1^{(i)}}{105\pi},$$

$$P_\gamma^{(i)} = \frac{3A_i^2}{4} + \frac{128(-1)^{i-1}A_iC_2}{105\pi} - \frac{256(-1)^{i-1}C_2\alpha_1^{(i)}}{315\pi}$$
$$- \frac{11}{4}A_i^2\Delta\Omega_{10}^{(i)} - \frac{256(-1)^{i-1}A_iM_1\Delta\Omega_{10}^{(i)}}{35\pi} - \frac{11}{4}A_i^2\Omega_1^{(i)}$$
$$- \frac{256(-1)^{i-1}A_iM_1\Omega_1^{(i)}}{35\pi} + 4A_i\alpha_1^{(i)}\Omega_1^{(i)}$$
$$+ \frac{256(-1)^{i-1}M_1\alpha_1^{(i)}\Omega_1^{(i)}}{21\pi},$$

$$N_3^{(i)} = \frac{3A_i^3}{4} + A_iC_1 + \frac{8(-1)^{i-1}A_i^2C_2}{3\pi} - \frac{3}{4}A_i^3\Omega_1^{(i)}$$
$$- A_iM_0\Omega_1^{(i)} - \frac{8(-1)^{i-1}A_i^2M_1\Omega_1^{(i)}}{3\pi},$$

$$E_\Omega^{(i)} = -\frac{A_i^3}{4} - \frac{8(-1)^{i-1}A_i^2M_1}{15\pi},$$

$$Q_\beta^{(i)} = -\frac{3A_i^2}{4} - C_1 - \frac{64(-1)^{i-1}A_iC_2}{21\pi} - \frac{9A_i\alpha_1^{(i)}}{4}$$
$$- \frac{1408(-1)^{i-1}C_2\alpha_1^{(i)}}{315\pi} + 9M_0\Delta\Omega_{10}^{(i)}$$
$$+ \frac{2048(-1)^{i-1}A_iM_1\Delta\Omega_{10}^{(i)}}{105\pi} + \frac{19}{4}A_i^2\Omega_1^{(i)} + 9M_0\Omega_1^{(i)}$$
$$+ \frac{2048(-1)^{i-1}A_iM_1\Omega_1^{(i)}}{105\pi} + \frac{19}{2}A_i\alpha_1^{(i)}\Omega_1^{(i)}$$
$$+ \frac{2944(-1)^{i-1}M_1\alpha_1^{(i)}\Omega_1^{(i)}}{105\pi} + \frac{19}{4}A_i^2\Delta\Omega_{10}^{(i)},$$

$$Q_\gamma^{(i)} = \frac{3A_i^2}{4} + C_1 + \frac{128(-1)^{i-1}A_iC_2}{45\pi} + \frac{3A_i\alpha_1^{(i)}}{2}$$
$$+ \frac{1792(-1)^{i-1}C_2\alpha_1^{(i)}}{495\pi} - 9M_0\Delta\Omega_{10}^{(i)}$$
$$- \frac{256(-1)^{i-1}A_iM_1\Delta\Omega_{10}^{(i)}}{63\pi} - 9M_0\Omega_1^{(i)}$$
$$- \frac{256(-1)^{i-1}A_iM_1\Omega_1^{(i)}}{63\pi} - 5A_i\alpha_1^{(i)}\Omega_1^{(i)}$$
$$- \frac{10496(-1)^{i-1}M_1\alpha_1^{(i)}\Omega_1^{(i)}}{495\pi} + \frac{5}{4}A_i^2\Omega_1^{(i)} + \frac{5}{4}A_i^2\Delta\Omega_{10}^{(i)},$$

$$N_4^{(i)} = \frac{A_i^3}{4} + \frac{8\,(-1)^{i-1}A_i^2 C_2}{15\pi} - \frac{1}{4}A_i^3\Omega_1^{(i)}$$
$$- \frac{8\,(-1)^{i-1}A_i^2 M_1\Omega_1^{(i)}}{15\pi},$$

$$F_\Omega^{(i)} = \frac{8\,(-1)^{i-1}A_i^2 M_1}{105\pi},$$

$$S_\beta^{(i)} = -\frac{3A_i^2}{4} - \frac{64\,(-1)^{i-1}A_i C_2}{45\pi} - \frac{3A_i\alpha_1^{(i)}}{4}$$
$$- \frac{128\,(-1)^{i-1}C_2\alpha_1^{(i)}}{3465\pi}$$
$$+ \frac{11}{4}A_i^2\Delta\Omega_{10}^{(i)} + \frac{2048\,(-1)^{i-1}A_i M_1\Delta\Omega_{10}^{(i)}}{315\pi}$$
$$+ \frac{11}{4}A_i^2\Omega_1^{(i)}$$
$$+ \frac{2048\,(-1)^{i-1}A_i M_1\Omega_1^{(i)}}{315\pi} + \frac{1}{2}A_i\alpha_1^{(i)}\Omega_1^{(i)}$$
$$- \frac{3712\,(-1)^{i-1}M_1\alpha_1^{(i)}\Omega_1^{(i)}}{693\pi},$$

$$S_\gamma^{(i)} = -\frac{3A_i^2}{4} - C_1 - \frac{640\,(-1)^{i-1}A_i C_2}{231\pi} - \frac{3A_i\alpha_1^{(i)}}{2}$$
$$- \frac{17152\,(-1)^{i-1}C_2\alpha_1^{(i)}}{5005\pi} + \frac{43}{4}A_i^2\Delta\Omega_{10}^{(i)}$$
$$+ \frac{32000\,(-1)^{i-1}A_i M_1\Delta\Omega_{10}^{(i)}}{693\pi} + \frac{43}{4}A_i^2\Omega_1^{(i)} + 25M_0\Omega_1^{(i)}$$
$$+ \frac{32000\,(-1)^{i-1}A_i M_1\Omega_1^{(i)}}{693\pi} + 5A_i\alpha_1^{(i)}\Omega_1^{(i)}$$
$$+ \frac{296704\,(-1)^{i-1}M_1\alpha_1^{(i)}\Omega_1^{(i)}}{15015\pi} + 25M_0\Delta\Omega_{10}^{(i)}.$$

$$N_5^{(i)} = -\frac{8\,(-1)^{i-1}A_i^2 C_2}{105\pi} + \frac{8\,(-1)^{i-1}A_i^2 M_1\Omega_1^{(i)}}{105\pi}.$$

REFERENCES

[1] W.-M. Zhang, H. Yan, Z.-K. Peng, and G. Meng, "Electrostatic pull-in instability in MEMS/NEMS: A review," *Sens. Actuators A, Phys.*, vol. 214, pp. 187–218, Aug. 2014.

[2] O. François and I. Dufour, "Enhancement of elementary displaced volume with electrostatically actuated diaphragms: Application to electrostatic micropumps," *J. Micromech. Microeng.*, vol. 10, no. 2, pp. 282–286, Jun. 2000.

[3] L. Yobas, D. M. Durand, G. G. Skebe, F. J. Lisy, and M. A. Huff, "A novel integrable microvalve for refreshable Braille display system," *J. Microelectromech. Syst.*, vol. 12, no. 3, pp. 252–263, Jun. 2003.

[4] C.-L. Dai, H.-L. Chen, and P.-Z. Chang, "Fabrication of a micromachined optical modulator using the CMOS process," *J. Micromech. Microeng.*, vol. 11, no. 5, pp. 612–615, Sep. 2001.

[5] S. Sadeghzadeh and A. Kabiri, "A hybrid solution for analyzing nonlinear dynamics of electrostatically-actuated microcantilevers," *Appl. Math. Model.*, vol. 48, pp. 593–606, Aug. 2017.

[6] J. Chen, J. Zou, C. Liu, J. E. Schutt-Aine, and S.-M. Kang, "Design and modeling of a micromachined high-Q tunable capacitor with large tuning range and a vertical planar spiral inductor," *IEEE Trans. Electron Devices*, vol. 50, no. 3, pp. 730–739, Mar. 2003.

[7] S. D. Senturia, *Microsystem Design*. New York, NY, USA: Springer, 2001, pp. 149–180.

[8] H. C. Nathanson, W. E. Newell, R. A. Wickstrom, and J. R. Davis, "The resonant gate transistor," *IEEE Trans. Electron Devices*, vol. ED-14, no. 3, pp. 117–133, Mar. 1967.

[9] K. B. Lee, "Closed-form solutions of the parallel plate problem," *Sens. Actuators A, Phys.*, vol. 133, no. 2, pp. 518–525, Feb. 2007.

[10] M. M. Joglekar and D. N. Pawaskar, "Estimation of oscillation period/switching time for electrostatically actuated microbeam type switches," *Int. J. Mech. Sci.*, vol. 53, no. 2, pp. 116–125, Feb. 2011.

[11] L. X. Zhang and Y.-P. Zhao, "Electromechanical model of RF MEMS switches," *Microsyst. Technol.*, vol. 9, nos. 6–7, pp. 420–426, Sep. 2003.

[12] Y. C. Hu, C. M. Chang, and S. C. Huang, "Some design considerations on the electrostatically actuated microstructures," *Sens. Actuators A, Phys.*, vol. 112, no. 1, pp. 155–161, Apr. 2004.

[13] L. M. Castaner and S. D. Senturia, "Speed-energy optimization of electrostatic actuators based on pull-in," *J. Microelectromech. Syst.*, vol. 8, no. 3, pp. 290–298, 1999.

[14] E. S. Hung and S. D. Senturia, "Generating efficient dynamical models for microelectromechanical systems from a few finite-element simulation runs," *J. Microelectromech. Syst.*, vol. 8, no. 3, pp. 280–289, 1999.

[15] J. I. Seeger and B. E. Boser, "Charge control of parallel-plate, electrostatic actuators and the tip-in instability," *J. Microelectromech. Syst.*, vol. 12, no. 5, pp. 656–671, Oct. 2003.

[16] J. A. Pelesko and X. Y. Chen, "Electrostatic deflections of circular elastic membranes," *J. Electrostatics*, vol. 57, no. 1, pp. 1–12, Jan. 2003.

[17] Y. Yu, L. Chen, Z. Wang, and G. Liu, "Response analysis of nonlinear free vibration of parallel-plate MEMS actuators: An analytical approximate method," *J. Vib. Eng. Technol.*, vol. 8, no. 6, pp. 935–946, Dec. 2020.

[18] B. Wu, W. Liu, X. Chen, and C. W. Lim, "Asymptotic analysis and accurate approximate solutions for strongly nonlinear conservative symmetric oscillators," *Appl. Math. Model.*, vol. 49, pp. 243–254, Sep. 2017.

[19] W. Liu, B. Wu, X. Chen, and W. Zhu, "Analytical approximate solutions for asymmetric conservative oscillators," *Arch. Appl. Mech.*, vol. 89, no. 11, pp. 2265–2279, Nov. 2019.

[20] B. S. Wu, Y. P. Yu, Z. G. Li, and Z. H. Xu, "An analytical approximation method for predicting static responses of electrostatically actuated microbeams," *Int. J. Non-Linear Mech.*, vol. 54, pp. 99–104, Sep. 2013.

W. J. LIU was born in Siping, China, in 1988. She received the B.S. degree in theoretical and applied mechanics and the Ph.D. degree in computational mathematics from Jilin University, China, in 2011, and 2017, respectively.

From 2017 to 2020, she held a postdoctoral position with the Guangdong University of Technology. From July 2018 to September 2018, she held a research assistant position at The Hong Kong Polytechnic University. Since 2020, she has been a Lecturer with the School of Mathematics and Computer Science, Jilin Normal University. She has published nine technical articles with a total of about 40 independent citations. Her research interests include the development of analytical approximate methods in engineering vibration, dynamic response of MEMS, and among others.

X. Q. ZHAO was born in Shanghai, China, in 1988. He received the B.S. degree in theoretical and applied mechanics and the Ph.D. degree in computational mathematics from Jilin University, China, in 2011 and 2018, respectively.

From 2018 to 2021, he held postdoctoral position at the Guangdong University of Technology. Since 2021, he has been a Lecturer with the School of Mathematics and Computer Science, Jilin Normal University. He has published seven technical articles with a total of more than 30 independent citations. His research interests include the efficient algorithms for frequency response and sensitivity analysis of large-scale systems, nonlinear vibration, structural topology optimization, and among others.

● ● ●